Supporting Information

Simultaneous Suppression of Shuttle Effect and Li Dendrite Growth by Light-Weight Bifunctional Separator for Li-S Batteries

*Seoa Kim[a‡], Won-Gwang Lim[a,b‡], Ara Cho[b‡], Jooyoung Jeong[a,b], Changshin Jo[c], DongGyu Kang[d], Seung Min Han[d], Jeong Woo Han[b], and Jinwoo Lee[a]**

[a] Department of Chemical and Biomolecular Engineering, Korea Advanced Institute of Science and Technology (KAIST), 291 Daehak-Ro, Yuseong-Gu, Daejeon 34141, Republic of Korea

[b] Department of Chemical Engineering, Pohang University of Science and Technology (POSTECH), 77 Cheongam-Ro, Nam-Gu, Pohang 37673, Gyeongbuk, Republic of Korea

[c] Institute for Manufacturing, Department of Engineering, University of Cambridge, 17 Charles Babbage Road, Cambridge, CB3 0FS, United Kingdom

[d] Department of Material Science and Engineering, Korea Advanced Institute of Science and Technology (KAIST), 291 Daehak-Ro, Yuseong-Gu, Daejeon 34141, Republic of Korea

‡ These authors contributed equally to this work

*Corresponding author. Tel: 82-42-350-3933; Fax: 82-42-350-3910; e-mail: jwlee1@kaist.ac.kr

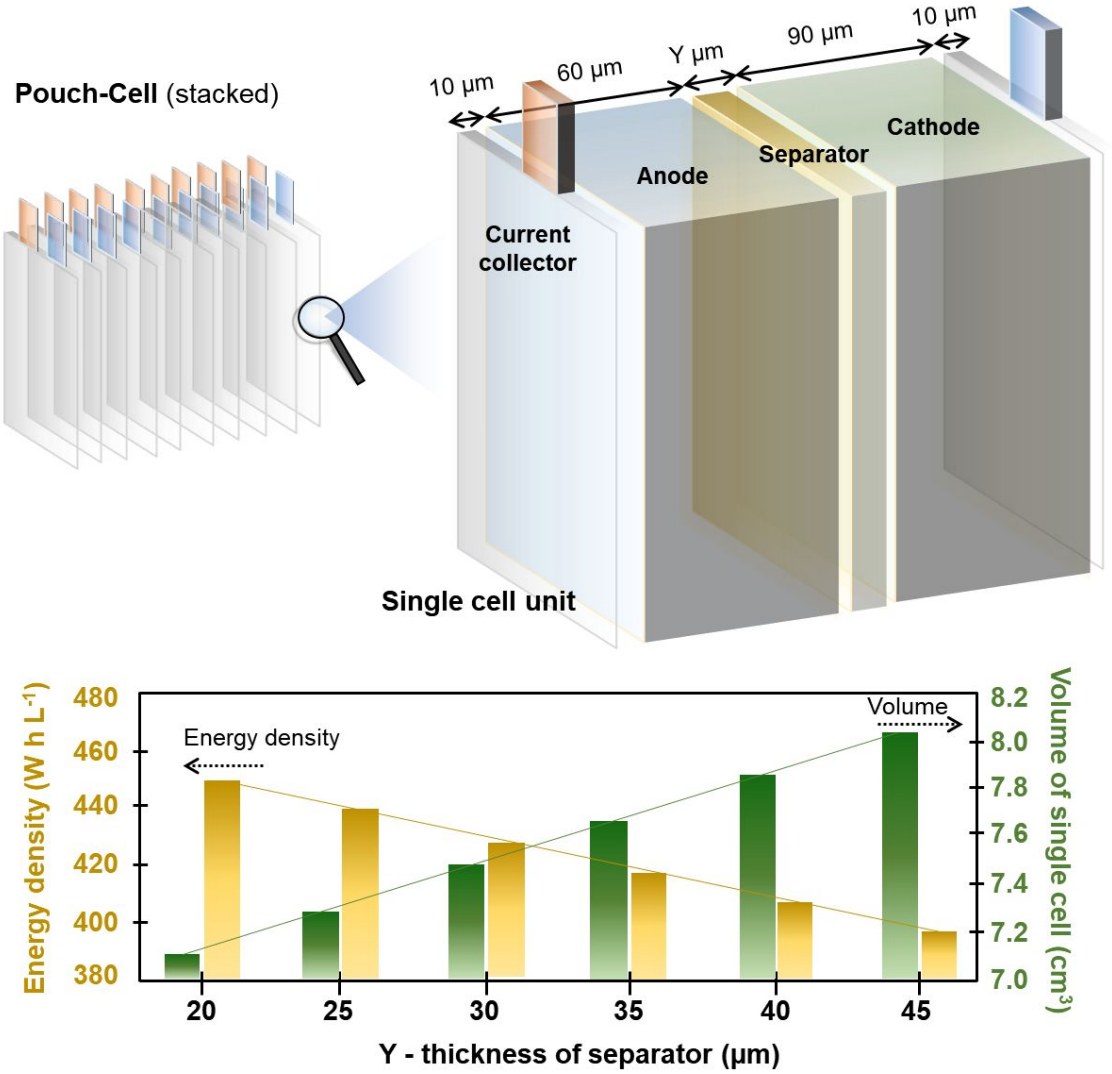

Figure S1. The configuration of Li-ion battery single cell unit and the energy density change with respect to the thickness of separator. The thickness of each part (current collector, anode, separator, and cathode) is determined based on conventional Li-ion battery. The thickness of separator and volumetric energy density of conventional Li-ion battery are assumed to 20 μm and 450 W h L^{-1}. The area of single cell unit is assumed to 375 cm^2.

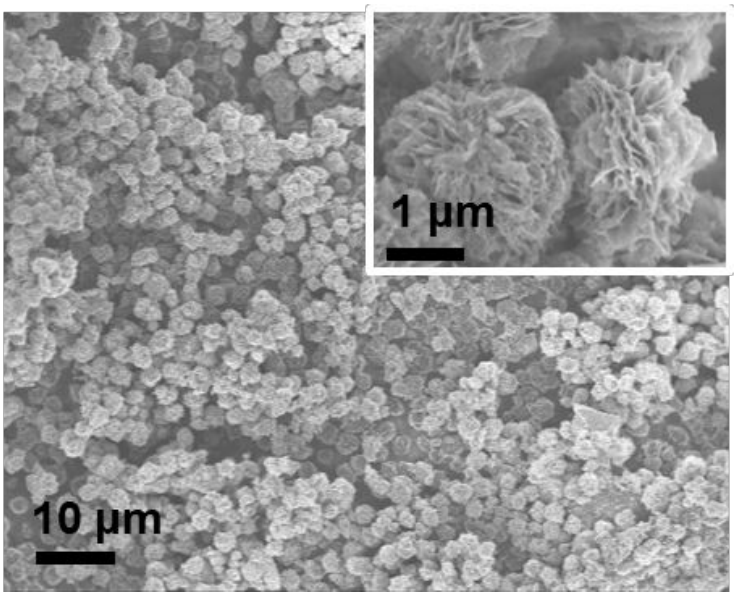

Figure S2. SEM images of f-Nb_2O_5 at different magnification.

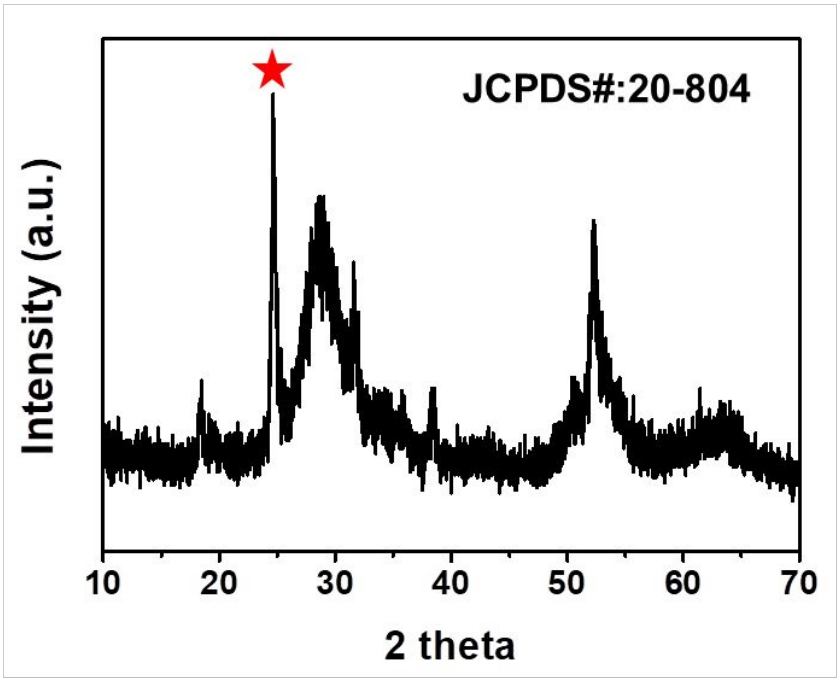

Figure S3. XRD pattern of orthorhombic f-Nb_2O_5. The marked peak corresponds to (113) plane.

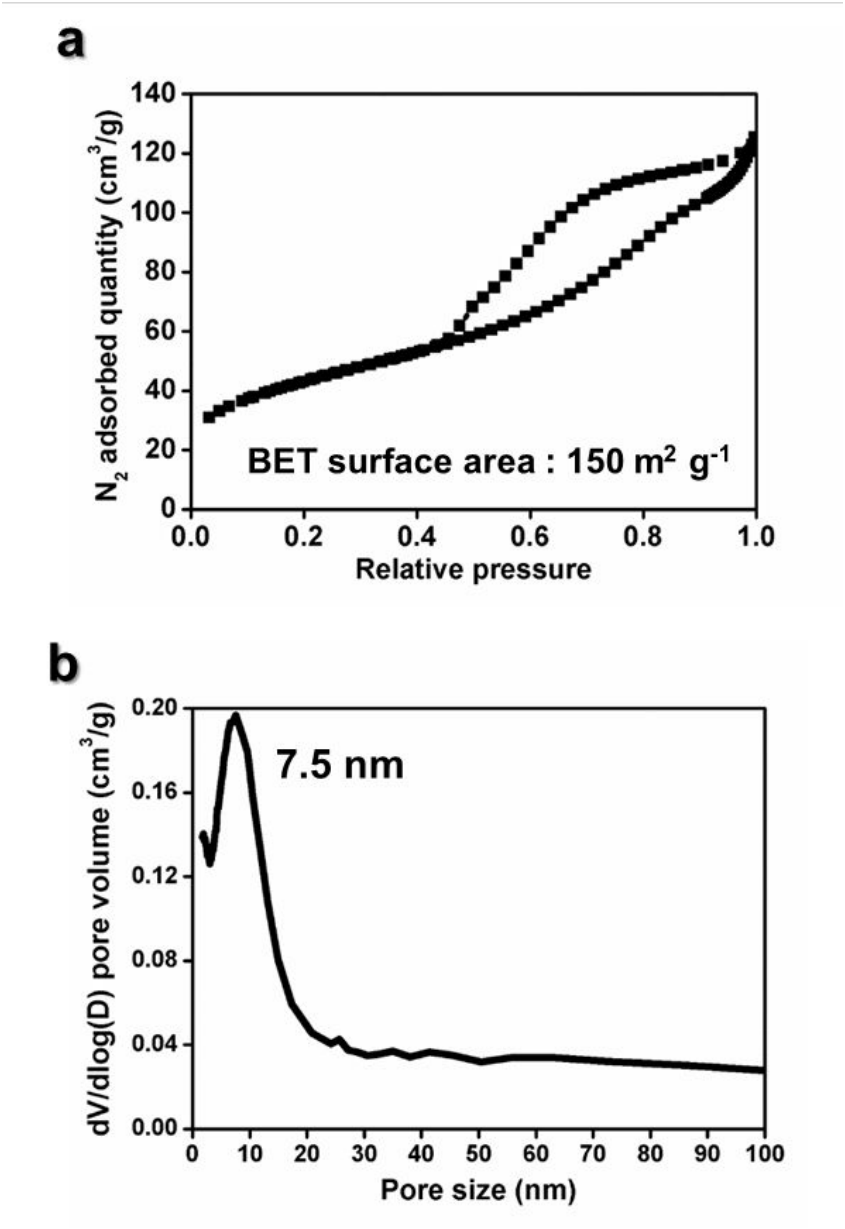

Figure S4. (a) Isotherm linear plot and (b) PSD of f-Nb_2O_5.

Figure S5. Phtographs of H-type cell using SP@PP separator.

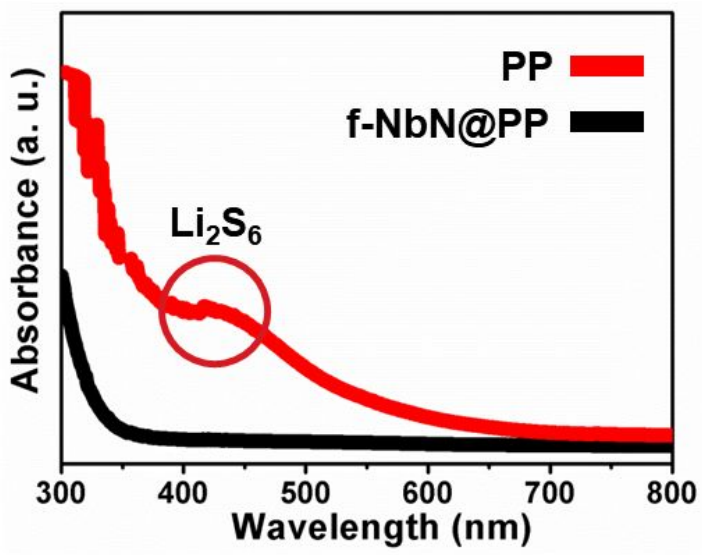

Figure S6. UV-visible adsorption spectra of anode chamber in H-type cell with PP and f-NbN@PP separator.

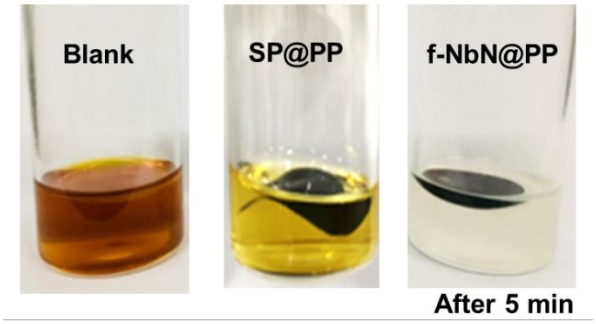

Figure S7. Static adsorption test of SP@PP and f-NbN@PP using LiPS solution (Blank).

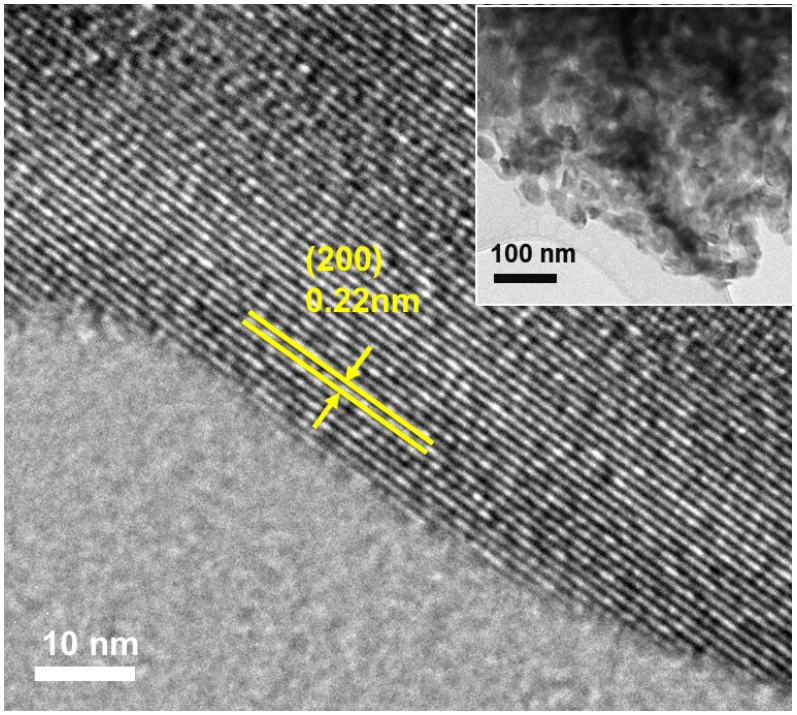

Figure S8. HR-TEM image of f-NbN.

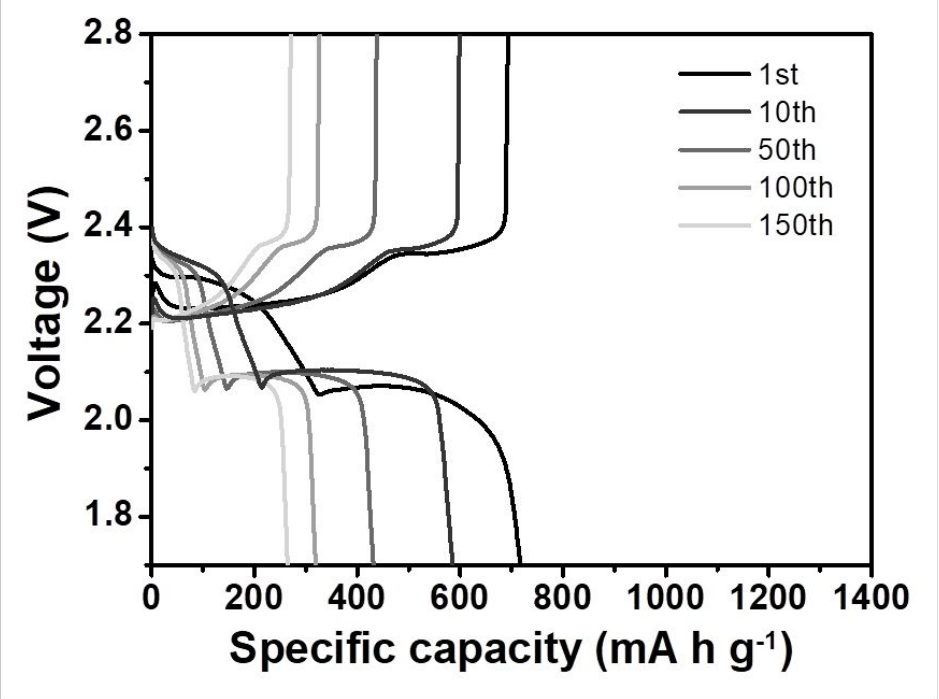

Figure S9. Voltage profile curve of SP+S//PP at 0.5 C rate.

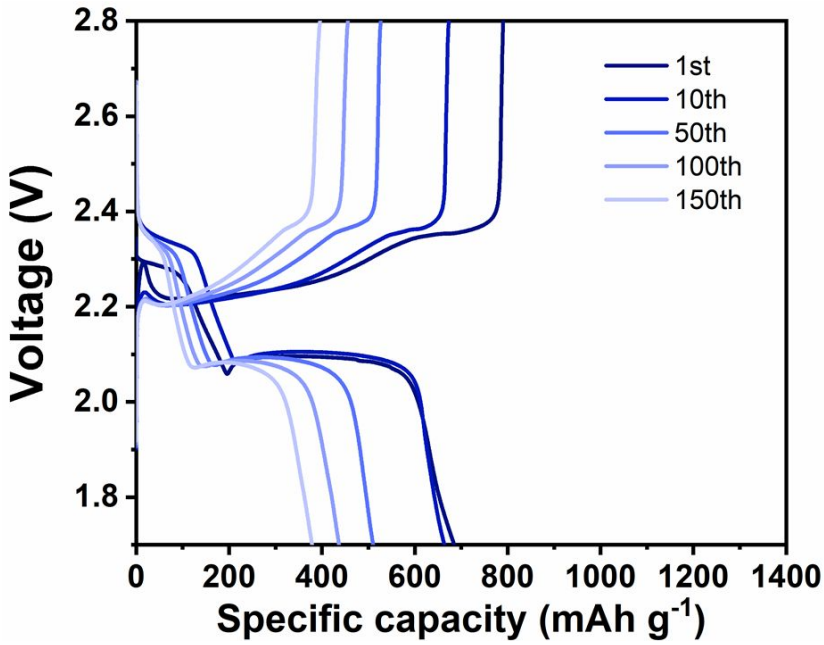

Figure S10. Voltage profile curve of SP+S//SP@PP at 0.5 C rate.

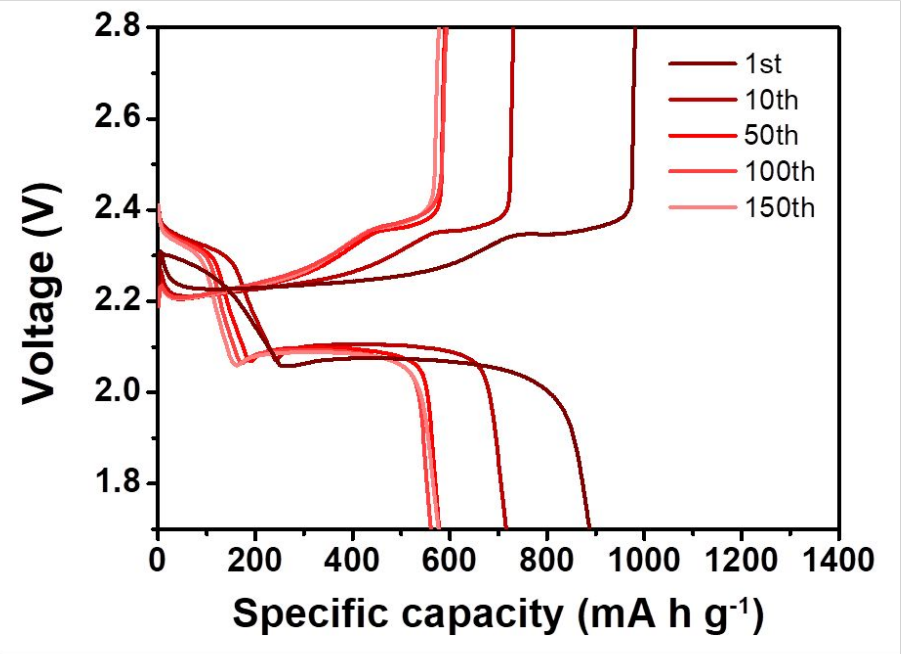

Figure S11. Voltage profile curve of SP+S//f-NbN@PP at 0.5 C rate.

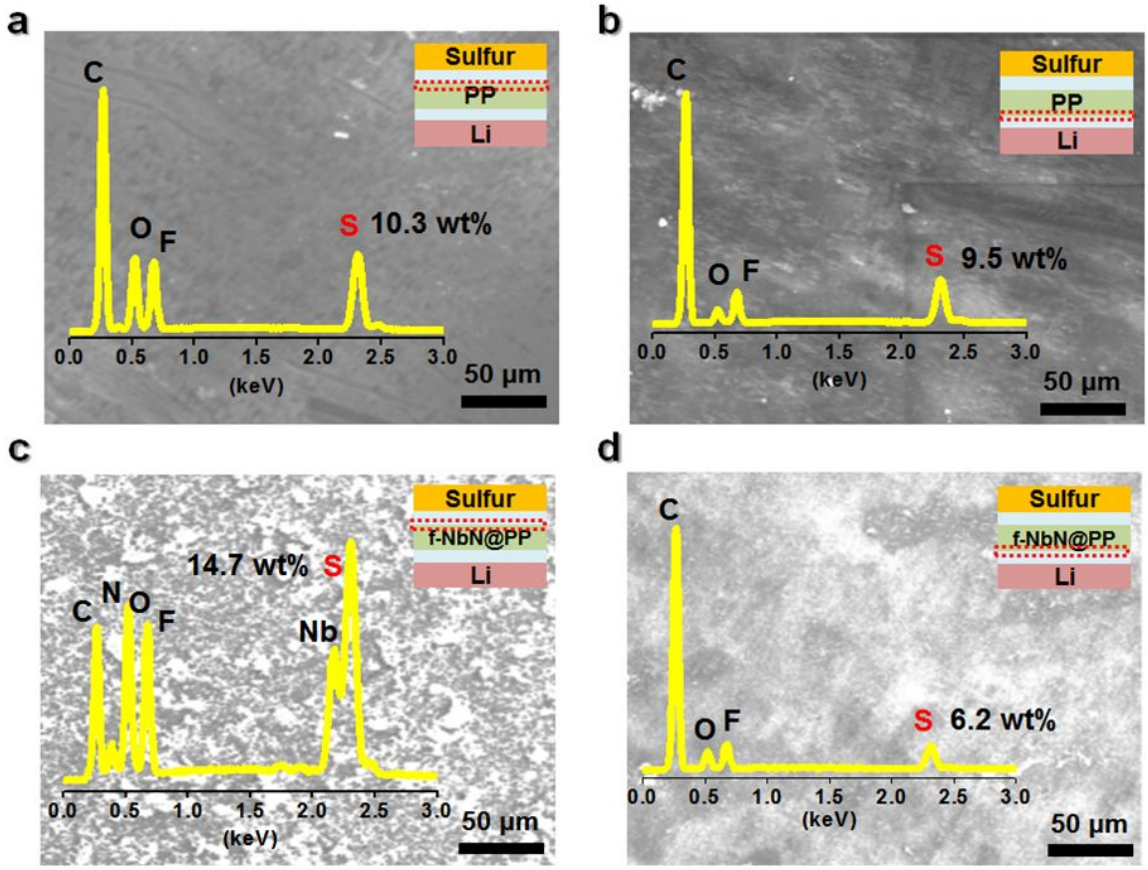

Figure S12. EDS analysis of (a) cathode side of PP, (b) anode side of PP, (c) cathode side of f-NbN@PP, and (d) anode side of f-NbN@PP after 150 cycles.

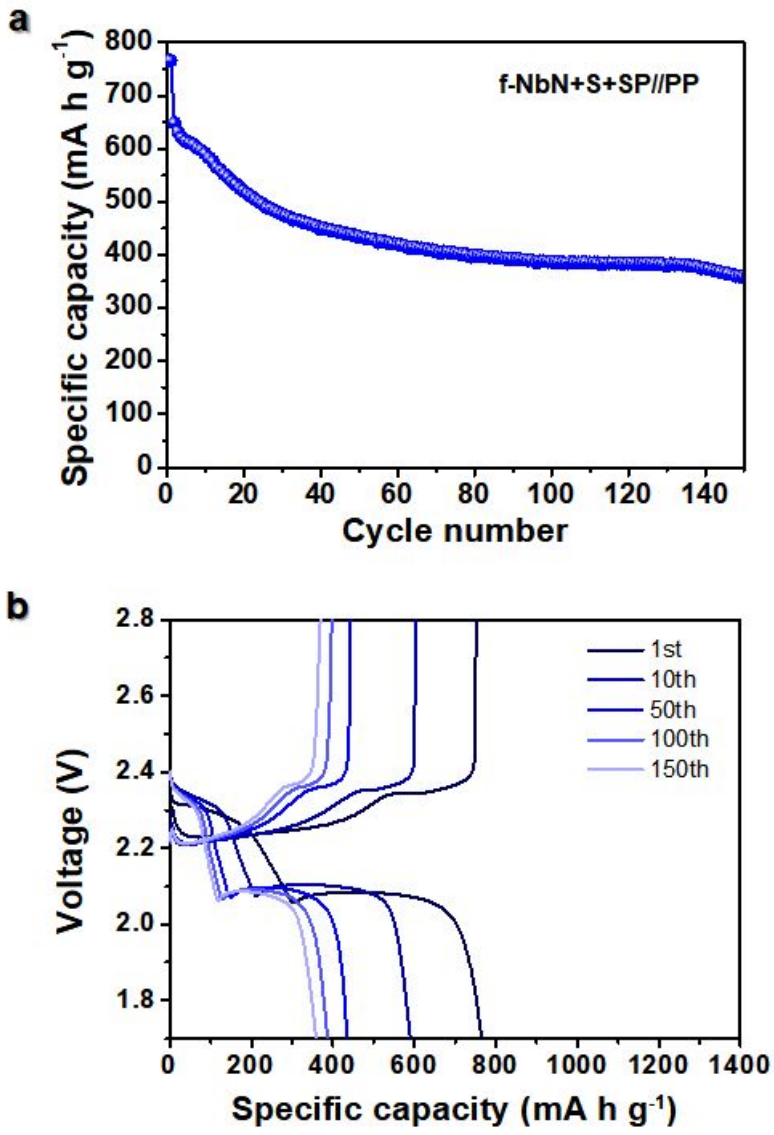

Figure S13. (a) Cycle performance and (b) voltage profile curve of f-NbN+S+SP//PP at 0.5 C rate.

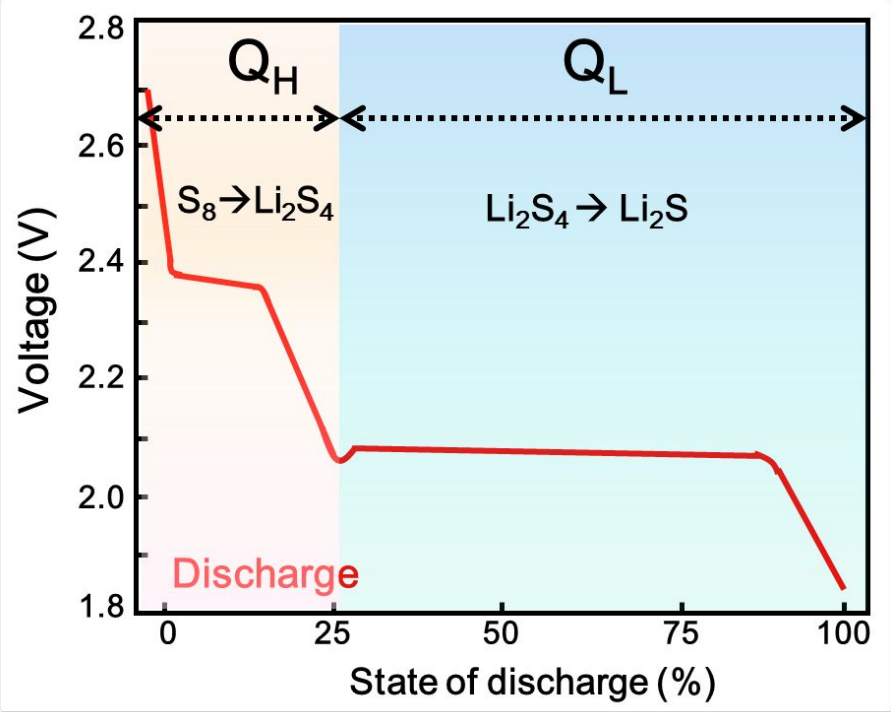

Figure S14. Schematic voltage profile curve of LSB during discharge process.

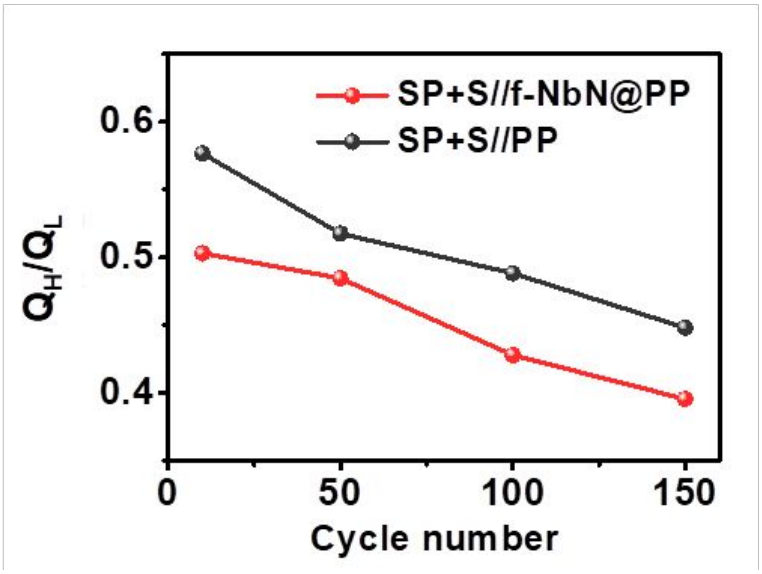

Figure S15. Q_H/Q_L values of SP+S/f-NbN@PP and SP+S//PP.

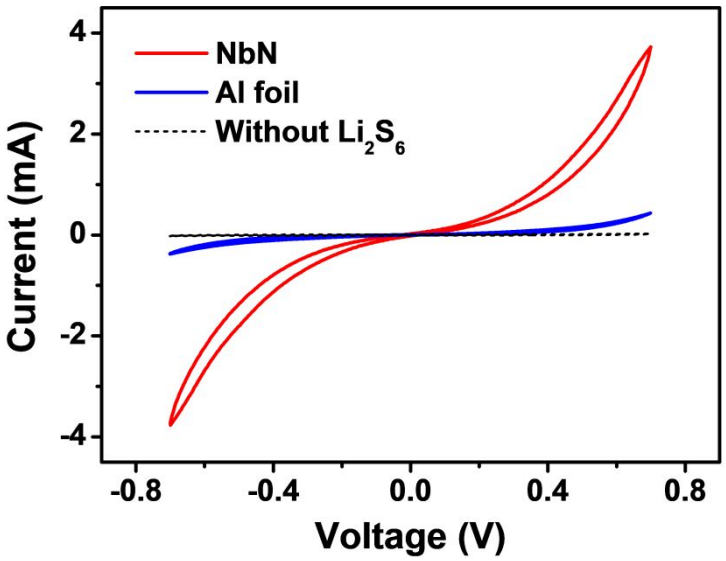

Figure S16. The CV curves of symmetric cells using Li_2S_6 catholyte.

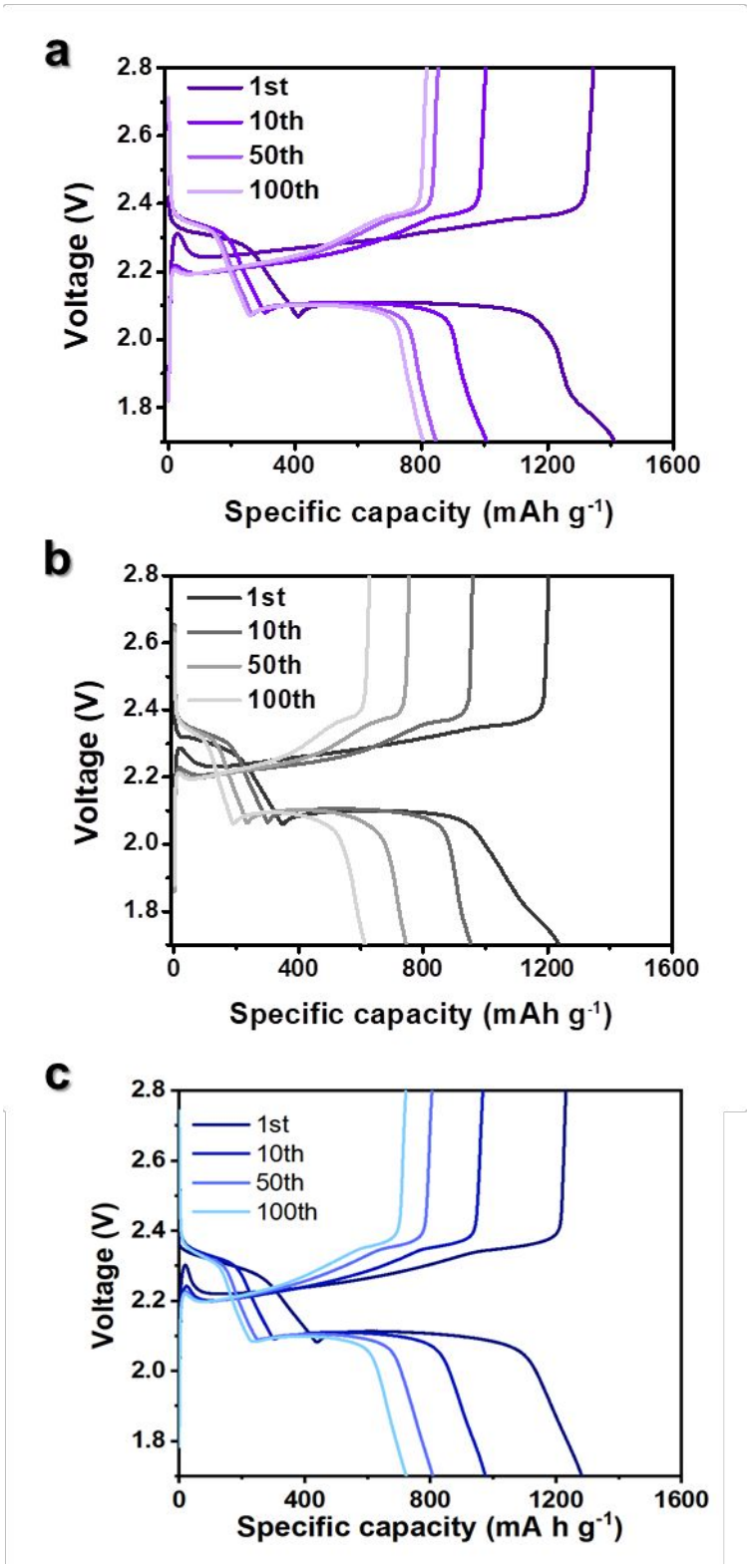

Figure S17. Voltage profile curves of (a) MCF+S//f-NbN@PP, (b) MCF+S//PP, and (c) MCF+S//SP@PP at 0.5 C rate.

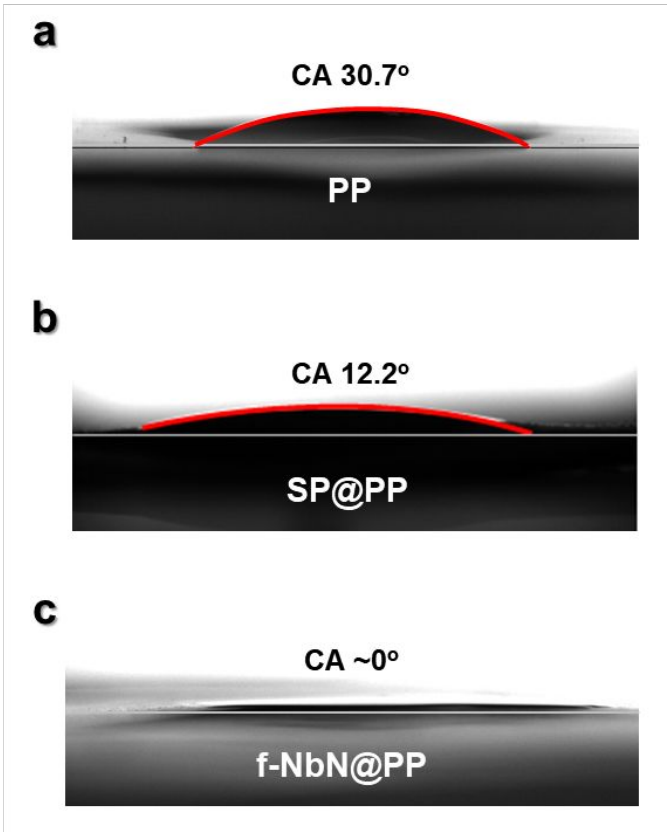

Figure S18. Contact angle measurement of (a) PP, (b) SP@PP, and (c) f-NbN@PP.

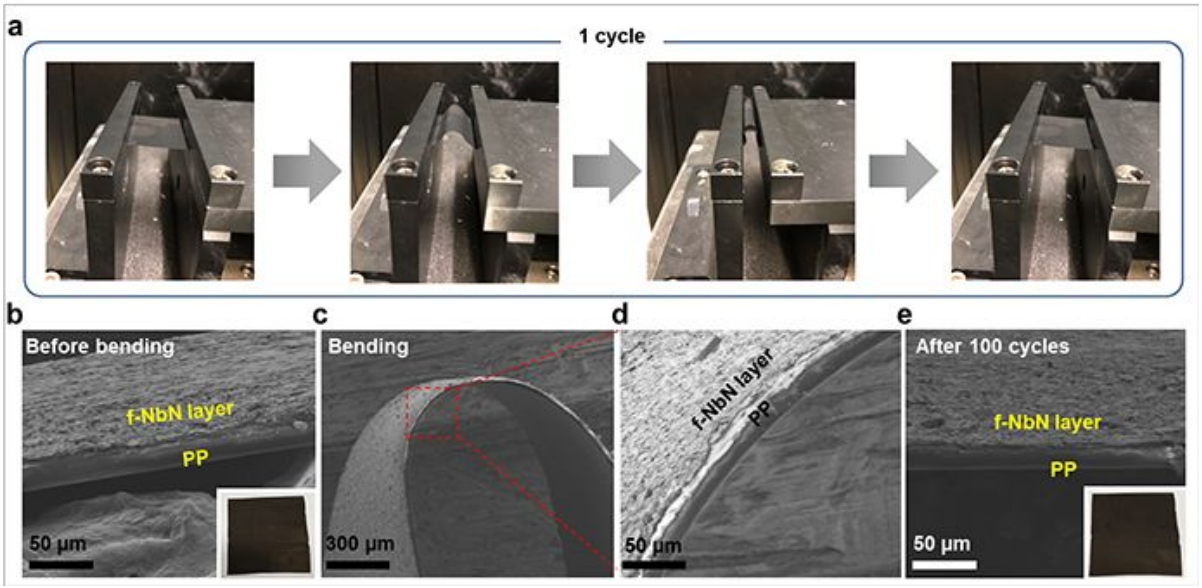

Figure S19. The bending stability test of f-NbN@PP. (a) Photographs of bending motion during 1 cycle. (b) SEM image and photograph (inset) of f-NbN@PP before bending. (c,d) SEM images of f-NbN@PP under different magnification after bending. (e) SEM image and photograph (inset) of f-NbN@PP after 100 cycles of repetitive bending motion.

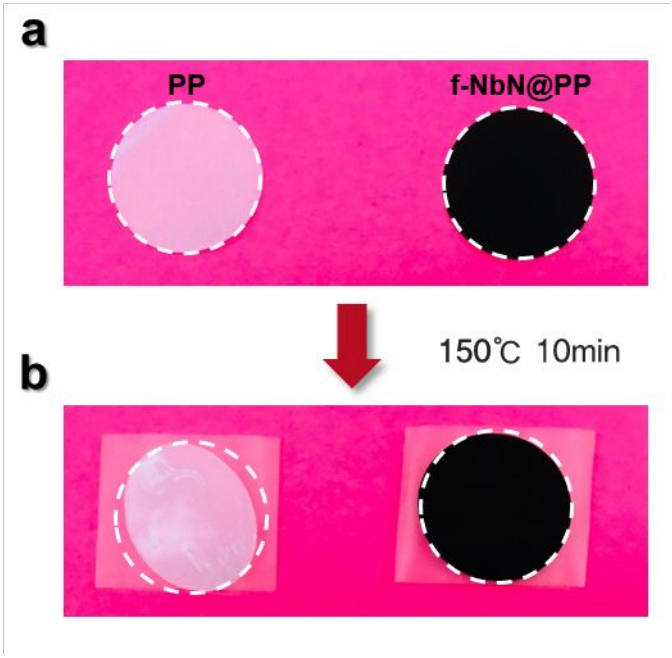

Figure S20. Thermal stability test of PP and f-NbN@PP separators. (a) Before and (b) after heating at 150 ^{o}C for 10 min.

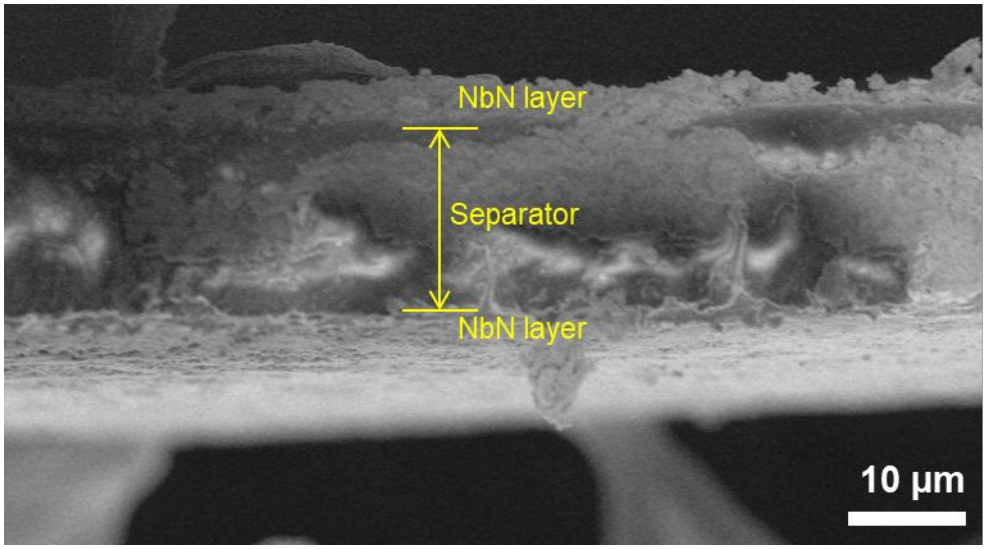

Figure S21. The SEM image of f-NbN@PP@f-NbN from the side view. The f-NbN layer is stably coated on the both side of separator.

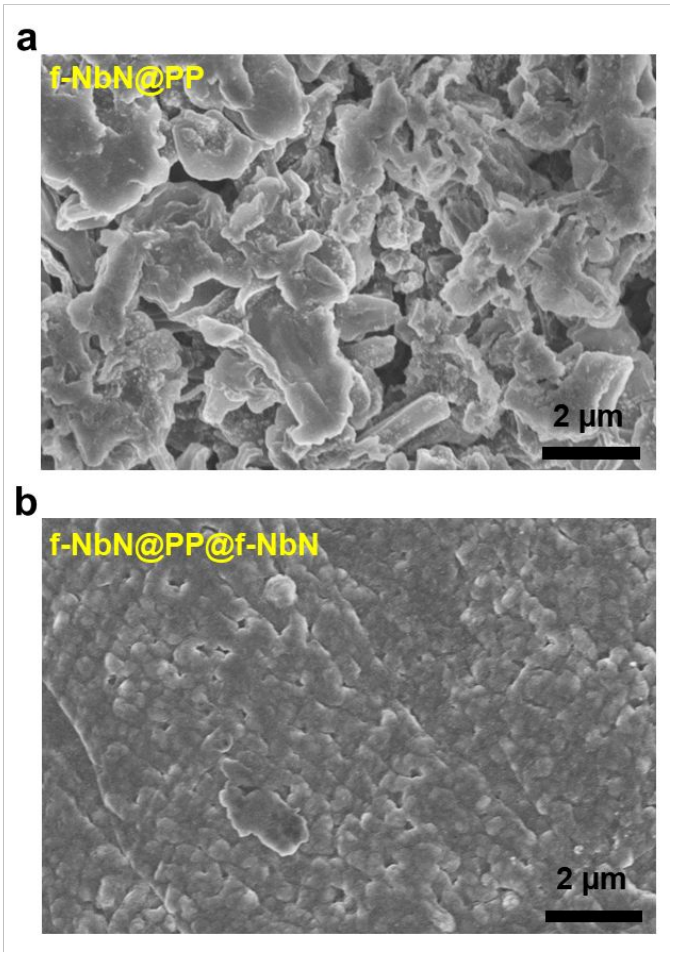

Figure S22. The top-view SEM images of Li metal after 50 cycles of LSB at 0.5 C rate, (a) with f-NbN@PP and (b) with f-NbN@PP@f-NbN. The cathode is faced with f-NbN layer and anode is faced with pristine PP in f-NbN@PP, while both cathode and anode are faced with f-NbN layer in f-NbN@PP@f-NbN. The electrolyte without the $LiNO_3$ additives was used to investigate the excessive growth of Li dendrite during charge/discharge process.

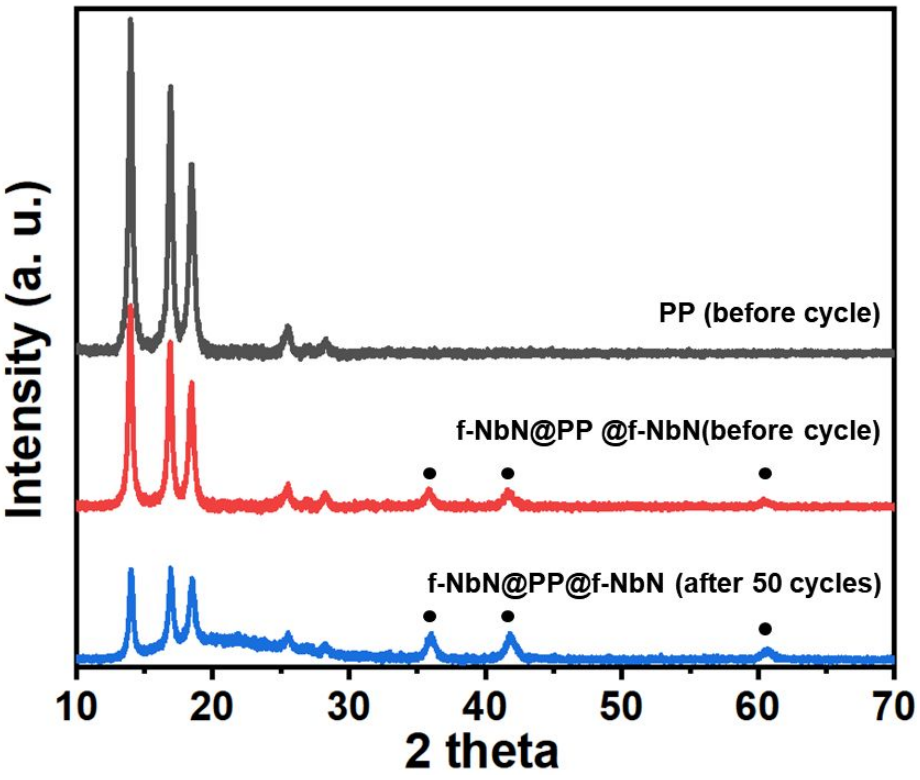

Figure S23. The XRD patterns of PP (before cycle), f-NbN@PP@f-NbN (before cycle), and f-NbN@PP@f-NbN (after 50 cycles). The peaks with black colored circle correspond to crystalline NbN and galvanostatic test was performed at 0.5 C rate.

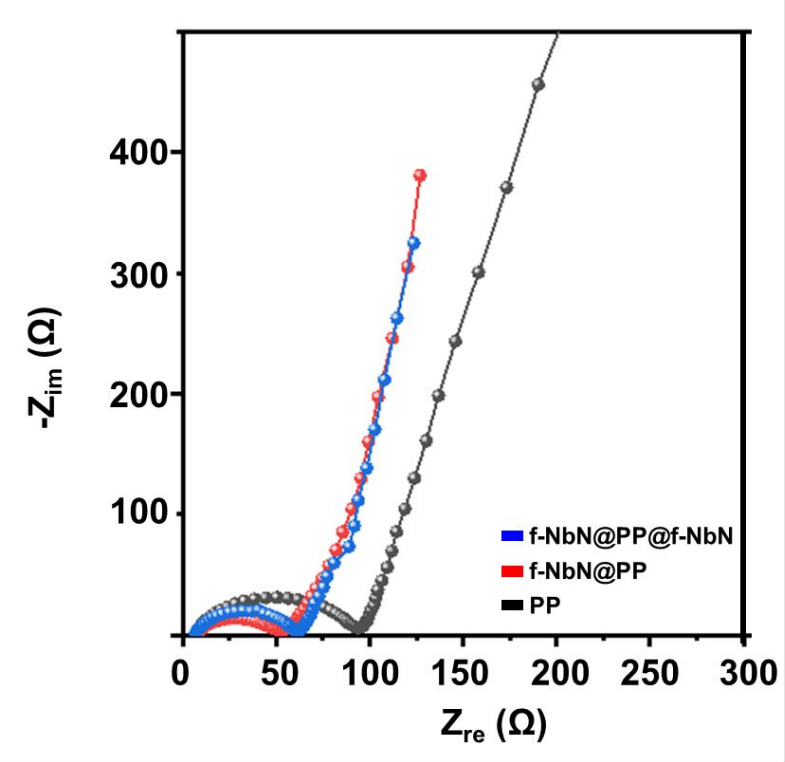

Figure S24. Nyquist plots of PP, f-NbN@PP, and f-NbN@PP@f-NbN with MCF+S electrode.

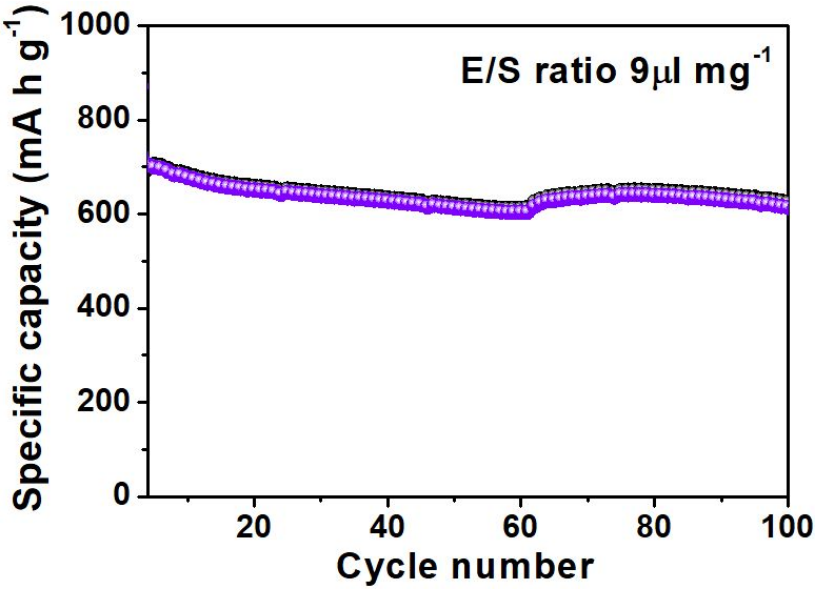

Figure S25. The cycle performance of MCF+S//f-NbN@PP@f-NbN at 1 C rate under E/S ratio of 9.